

# Geophysical Research Letters

## RESEARCH LETTER

10.1029/2020GL089639

## A New Technique for Investigating Dust Charging in the PMSE Source Region

Alireza Mahmoudian<sup>1</sup> , Mike J. Kosch<sup>2,3,4</sup> , Juha Vierinen<sup>5</sup> , and Michael T. Rietveld<sup>5,6</sup> 

<sup>1</sup>Institute of Geophysics, University of Tehran, Tehran, Iran, <sup>2</sup>Department of Physics, Lancaster University, Lancaster, UK, <sup>3</sup>South African National Space Agency (SANSA), Hermanus, South Africa, <sup>4</sup>Department of Physics and Astronomy, University of the Western Cape, Bellville, South Africa, <sup>5</sup>Department of Physics and Technology, University of Troms, Troms, Norway, <sup>6</sup>EISCAT Scientific Association, Ramfjordmoen, Norway

### Key Points:

- First radio modulation of PMSE source region with varying HF pump power is presented
- Direct observation of dust charging in the mesosphere through controlled  $T_e/T_i$  is observed
- Power stepping and continuous power sweeping can be used for charge state validation and saturated charge state determination, respectively

### Correspondence to:

A. Mahmoudian,  
a.mahmoudian@ut.ac.ir

### Citation:

Mahmoudian, A., Kosch, M. J., Vierinen, J., & Rietveld, M. T. (2020). A new technique for investigating dust charging in the PMSE source region. *Geophysical Research Letters*, 47, e2020GL089639. <https://doi.org/10.1029/2020GL089639>

Received 4 JUL 2020

Accepted 17 SEP 2020

Accepted article online 21 SEP 2020

**Abstract** A new technique for investigating dust charging in the PMSE (polar mesospheric summer echoes) source region is proposed and discussed in this paper. The first high-frequency (HF) modulation of the PMSE with varying pump power was employed during a recent experimental campaign at EISCAT (European Incoherent Scatter Scientific Association). Two experiment setups including HF pump power stepping as well as quasi-continuous power sweeping were used. The experiment was designed based on a computational model capable of simulation of PMSE evolution during HF pump modulation in order to develop a new approach for studying the dust charging process in the PMSE source region. The charge state of dust particles along with background dusty plasma parameters is estimated using the experimental and computational results. A detailed future experimental design based on background dusty-plasma parameters is proposed.

## 1. Introduction

Polar mesospheric summer echoes (PMSE) are very strong radar echoes observed in the frequency range of 2 MHz up to 1 GHz (Cho & Rottger, 1997; Ecklund & Balsley, 1981; Rapp & Lubken, 2004). PMSEs are coherent echoes produced by plasma (electron density) fluctuations at half the radar wavelength (known as Bragg scattering condition) (Rapp & Lubken, 2004).

The first modulation of PMSE by high-power radio waves was examined in 2000 and 2003 (Chilson et al., 2000; Havnes et al., 2003). Subsequently, the computational models were developed to study the associated physics of such experiments and explain the observational data (Chen & Scales, 2005; Mahmoudian et al., 2018; Scales, 2004; Scales & Mahmoudian, 2016). Considering the model prediction of the different behavior of PMSE at the HF band (e.g., 8 MHz) and VHF (e.g., 224 MHz), a simultaneous experiment using the two radars was conducted at EISCAT in 2013 for the first time (Senior et al., 2014). The diffusion and electron attachment onto the dust particles (dust charging) are the two processes that control the electron density fluctuation amplitude and the corresponding radar echoes (Scales & Mahmoudian, 2016). The dust charging ( $\tau_{\text{chg}}$ ) and diffusion ( $\tau_{\text{diff}}$ ) time period can be written as follows (Scales & Mahmoudian, 2016):

$$\tau_{\text{chg}} = \frac{1}{|I_e + I_i|} \approx \frac{1}{\sqrt{8\pi} r_d^2 v_{te0} \sqrt{r_h} e^{\frac{\phi}{r_h}}}, \quad (1)$$

$$\tau_{\text{diff}} \approx \frac{\lambda_{\text{irreg}}}{2\pi} \frac{1}{\frac{KT_i}{m_i v_{in}} (1 + r_h) \left(1 + \frac{Z_{d0} n_{d0}}{n_{e0}}\right)}, \quad (2)$$

where  $\lambda_{\text{irreg}}$ ,  $K$ ,  $T_i$ ,  $m_i$ ,  $v_{in}$ ,  $Z_{d0}$ ,  $n_{d0}$ ,  $n_{e0}$ ,  $r_d$ ,  $v_{te0}$ ,  $\phi$ , and  $r_h$  denote electron density fluctuation wavelength, Boltzmann constant, ion temperature, ion mass, ion neutral collision frequency, dust charge number, dust number density, electron number density, dust radius, electron thermal velocity, equilibrium normalized dust floating potential, and heating ratio ( $T_e/T_i$ ), respectively.

As shown in Equations 1 and 2, both processes depend on electron temperature ( $T_e$ ); therefore, radio modulation of PMSE will modify the two processes (Scales & Mahmoudian, 2016). Background dusty plasma parameters also play a role in the diffusion and charging timescales. The diffusion process is proportional to

the radar frequency. While the VHF PMSE in the conventional PMSE heating experiments at fixed power can be used as a manifestation of dust charging process, the study of the dust charging process and estimation of the dust floating potential, dust charge state, and its variation during pump heating is impossible using the conventional observations. To study the dust charging process based on the parameters presented in Equations 1 and 2, the common region within the PMSE should be probed by radar between different cycles. While most of the past experiments focused on multiple radar frequencies in order to distinguish the diffusion/charging processes during radio modulation ( $T_e/T_i$  variation), due to altitude difference of reflected echoes and changes in the background dust and plasma parameters (radius and density) such a comparison had a low accuracy. The recent simultaneous observations of modulated PMSE at 56 and 224 MHz have shown similar limitations as the probed region by the two radars is not common and encompass different background dust parameters (Havnes et al., 2015). The previous study has shown the 8 MHz radar signal undergoes a significant absorption during heating, which makes discriminating the effect of charging and study charging process almost impossible (Senior et al., 2014). Therefore, the present work is designed based on our extensive work on studying the physics of PMSE modulation with radio waves. We used the most reliable radar frequency (224 MHz) to determine the altitude range of study between experiments and have the constant dust parameters over a short period of experiments and only have  $T_e/T_i$  variation between cycles. The continuous and stepped pump power variation are employed in order to not only facilitate the first direct observation of dust charging process but also to determine charge state, background dust parameters, and dust charge variation in response to the heating. The continuous pump heating has clearly shown the saturation of the dust charging process at some levels of pump power, which is essential in determining the dust charging rate and saturation level, initial dust charge state and its time evolution, and background parameter estimation.

## 2. Experimental Setup

The HF pump modulation campaign was conducted from 22–26 July 2019 at the EISCAT site near Troms, in northern Norway. The experiments started around 7:00 UT every day and continued to ~13:00 UT based on the mesospheric conditions and presence of a PMSE layer. The VHF data presented in this paper have a vertical resolution of 300 m and a time resolution of 4.8 s, which corresponds to the integration time of the autocorrelation functions of the radar echo. The modulation scheme used was a pulse-to-pulse correlation manda.

The HF facility was used both as a heater of electrons in the mesosphere together with the VHF radar observations (Rietveld et al., 2016). Ten transmitters were used with Antenna Array 1 at 6.2 MHz, vertical beam, X-mode for the 3 days presented below. A short summary of the experiment conducted on each day is provided below.

July 24: The HF experiment ran with X-mode heating, and this certainly gave very good PMSE modulation as will be discussed shortly. Power was stepped up between 40, 60, and 80 kW for the first part and changed subsequently to 10, 20, 40, 60, and 80 kW for each new heating cycle in the last hour of the experiment. The nominal power per transmitter of 20, 40, 60, and 80 kW for each new heating cycle corresponds to effective radiated powers (total transmitter power times antenna array gain, ERP) of approximately 52, 114, 240, 380, and 485 MW, respectively, assuming a perfectly conducting ground. The heater was on for 48 s followed by 120 s off period.

July 25: The first hour of experiment showed a very weak VHF PMSE. Around 09:38 UT, the VHF echo started to form and the HF modulation started at 20, 40, 60, and 80 kW for each new heating cycle. Around 09:40 UT, VHF PMSE got much stronger, at a high altitude of about 88 km. The experiment continued until 11:00 UT. The HF transmitter was configured for X-mode polarization at 6.2 MHz. In order to make sure that the HF off time was long enough to avoid preheating condition in the following heating cycle, the heater off time was increased to 144 s giving a 192 s total cycle.

July 26: In the last day of experiment, the heating power actually increased during the cycle continuously. The VHF radar started at 07:00 UT and ran until the scheduled end of 11:00 UT. There were PMSE echoes, which were stable in the first 2 hr, but not too strong. The 62.4 s heater on cycle with linear power sweep started at 07:19 UT. The HF experiment ran with X-mode heating again. For almost the first 2 hr, the HF heater ran with a linear power sweep from 0 to full power in 62.4 s during the cycle followed by 144 s off giving a 206.4 s cycle. In order to provide a scientific-based experiment design to investigate dust charging

process in the Earth's middle atmosphere, a quasi-continuous power stepping is implemented, which uses many small steps every 0.515 s, rather than the power stepping over on/off cycles. Specifically, the power of the 10 heating transmitters was increased in 120 steps (giving 62.4s on period) from 0 to 80 kW nominally per transmitter followed by 144s off. At around 09:02 UT the experiment was changed to the same power stepping program as on 25 July. In the second half of the run, the VHF PMSE became weaker and more variable and was sometimes absent.

### 3. Observations

The experimental observations associated with the 3 days discussed in the previous section are presented. Figure 1a shows that the natural VHF PMSE layer started at 07:21:26 UT on 24 July 2019 with a single structure expanded from ~81 to 84 km. The HF pump modulation of PMSE started at 07:46:20 UT. The HF pump power was set to 40, 60, and 80 kW. A very weak modulation of VHF PMSE associated with the pump power of 40 kW is observed (Figures 1a and 1b). A large weakening of VHF PMSE during HF heating at 60 kW and almost complete disappearance of the modulated PMSE at 80 kW are observed in the VHF radar data. The heating continued until 08:36:44 UT when the natural PMSE became very weak. At 09:10:20 UT, a double layer PMSE started to form. The first layer has a thickness of ~3 km (81.5–84.5 km), and a narrow PMSE layer of ~1 km appeared at a center altitude of 88.11 km. The very interesting modulation effects and similar characteristics of the VHF PMSE described for Figure 1a are observed at both PMSE layers with an altitude difference of ~5 km. A clear radio-wave modulation at the top PMSE layer can be seen. This will be elaborated using the modeling results in following section.

Figure 1c shows the experimental observations collected on 25 July 2019. The VHF PMSE data from 09:37:36 to 10:59:50 UT are presented. The HF pump transmitter was operated at four power levels of 20, 40, 60, and 80 kW. The clear modulation and agreement of VHF PMSE associated with the power level, which is expected to decrease proportionally to heating ratio ( $T_e/T_i$ ) and increase of pump power, are observed (Scales & Mahmoudian, 2016). The physics of VHF PMSE variation during radio-wave heating will be explained using the numerical simulations in the following section. The more detailed analysis including superposed-epoch analysis of the averaged signal over altitude (~80.91–84.51 km) is shown in Figure 2c for the heating cycles 09:53:36–10:19:16 UT. Three power levels of 40, 60, and 80 kW are presented. The agreement of the amplitude reduction of the normalized radar echoes during heating and turn-off overshoot with the HF pump power will be elaborated in section 3. Another case from 24 July 2019 between 10:00:48 and 10:14:48 UT (80.91–84.51 km) is also included in Figure 2d in order to address the lower pump power modulation that is dependent on the background dusty plasma parameters.

The superposed-epoch analysis of the VHF radar echoes associated with several heating time intervals on 24 July 2019 (Figure 1) are presented in Figures 2a and 2b. The subinterval analysis corresponds to averaged power over the altitude of the PMSE layer and normalized for the time period of heater on and off at each HF transmitter power. Figures 2a and 2b represent the above-mentioned analysis for the PMSE layer formed in the lower altitude range of ~82–84 km in two successive heating cycles. The normalized radar echoes are very consistent for both cycles with the same suppression amplitude, turn-off overshoot, and relaxation time at HF heating powers of 40, 60, and 80 kW. Considering the short time period as well as overall behavior of the PMSE layer in the VHF data that is related to the background dusty plasma parameters, this behavior emphasizes the similar HF modulation and heating effects on the layer. The results of the superposed-epoch analysis denote the time variation of the PMSE layer and different effect of HF pump heating on the layer.

The experimental observations in Figure 3a show the 62.4 s heating cycle with quasi-continuous power stepping (denoted by on) on 26 July 2019. It is clear that as the power starts at a very low amplitude, the persistence of PMSE strength from the off cycle extends to the new heating cycle. As the power increases and the  $T_e/T_i$  grows to larger values, the scattered radar signal drops significantly toward the end of heating cycle. The suppression of the weak PMSE layer for heating cycles after 08:41:04 UT even appears right after heater turn-on. The subintervals at each power step are analyzed by performing a superposed-epoch analysis of the Radar Cross Section (RCS) from the radar over the heating cycles. The associated superposed-epoch analysis of Figure 3a is shown in Figure 3b. The clear modulation behavior described for Figure 3a is seen. The averaged VHF PMSE over all heating cycles is shown in Figure 3c. According to this figure, a slow decrease of echo strength by about 80% is observed. Unlike the instant modulation of PMSE layer with radio waves explained for experiments on 24 and 25 July, the slow increase of HF pump power from zero to 80 kW

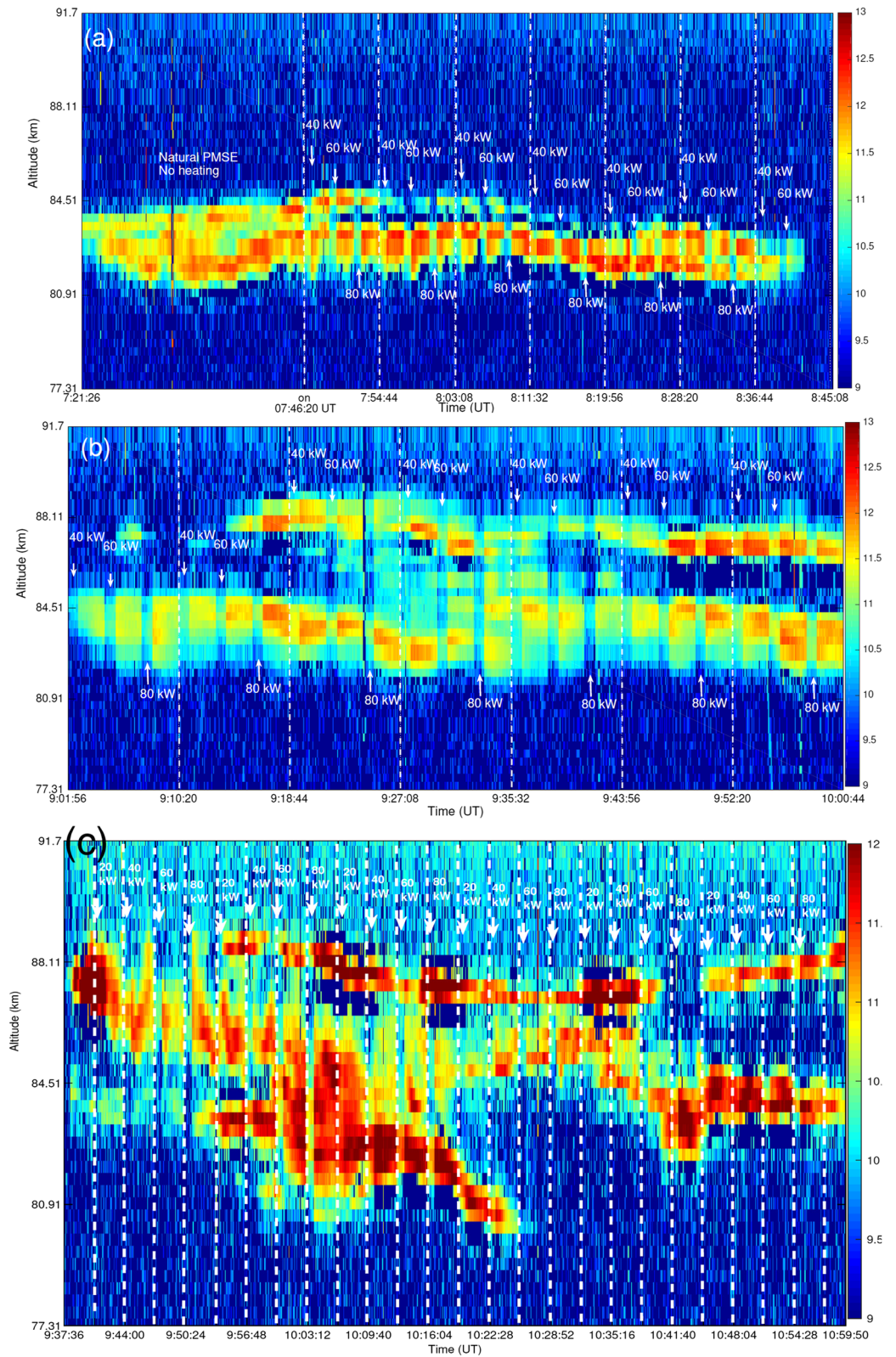


**Figure 1.** (a and b) The VHF PMSE during radio-wave modulation including HF power variation over the heating cycles on 24 July 2019. The powers shown are the nominal power radiated by each of the 10 transmitters. (c) The VHF PMSE during radio-wave modulation including HF power variation with increased off period and total heating cycle of 192 s on 25 July 2019. The backscattered signal is shown in  $\log_{10}(N_e)$  units.



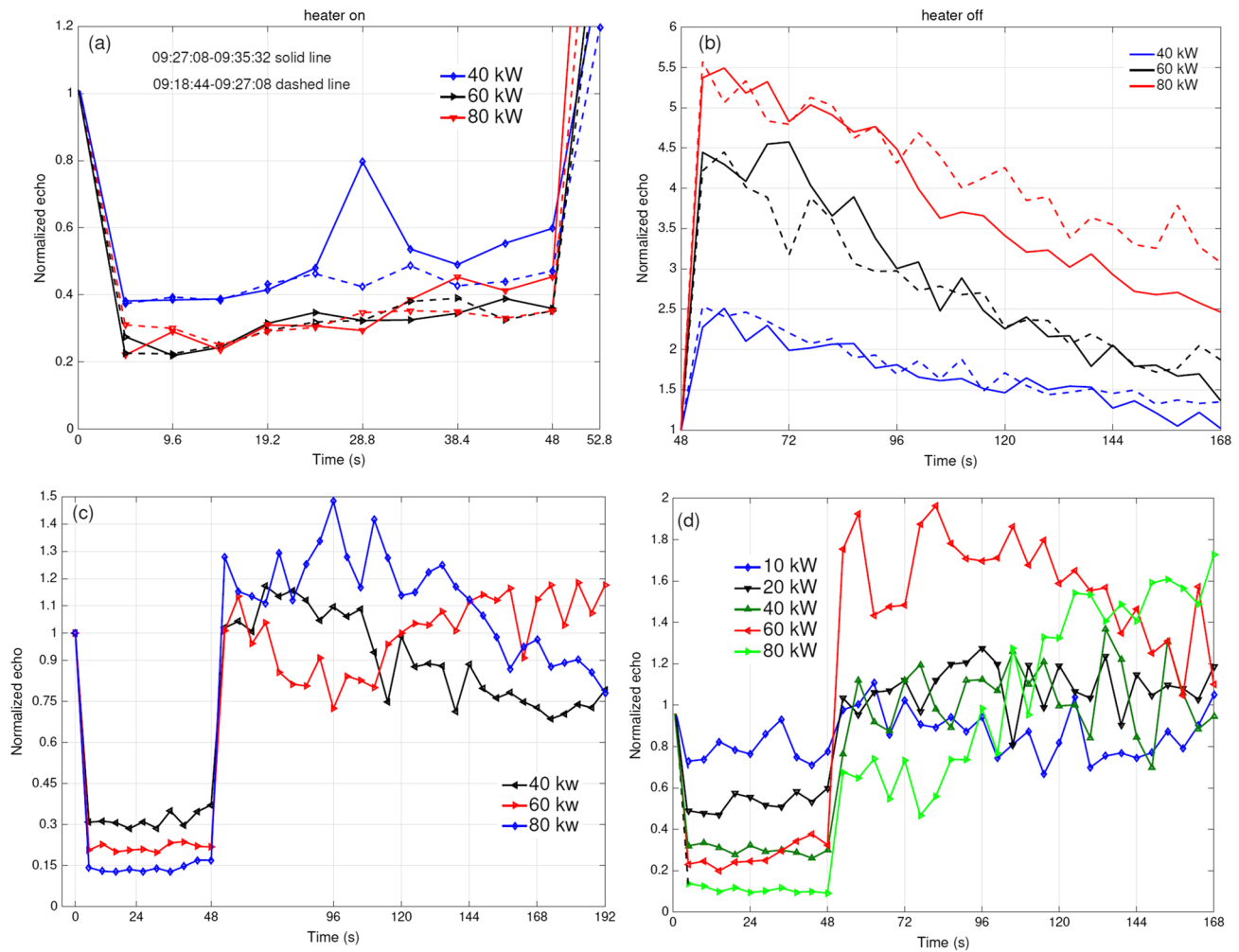


**Figure 2.** Subintervals at each power step analyzed by performing a superposed-epoch analysis of the RCS (radar cross section) over the heating cycles. (a) Turn-on and (b) turn-off normalized radar echoes associated with the bottom layer in the altitude range of 82.7–84.5 km and 82.35–83.49 km corresponding to 09:18:44–09:27:08 UT and 09:27:08–09:35:32 UT time intervals, respectively, on 24 July 2019. (c) Corresponds to 09:53:36–10:19:16 UT and average altitude range of 80.91–84.51 km on 25 July 2019. (d) Corresponds to 10:00:48–10:14:48 UT and average altitude range of 80.91–84.51 km on 24 July 2019.

in 62.4 s represents a different behavior of associated VHF PMSE. A slow decay denotes the slow charge state variation of dust particles in response to  $T_e/T_i$  increase over small steps. This behavior is noted as a plateau within  $\sim 10$  s (Figure 3c). A saturated charging process after 38.4 s of the heating cycle is seen with less than 10% variation in the radar echo. The corresponding physics will be elaborated in the subsequent section and by implementing the numerical simulations.

#### 4. Diagnosis of Dust Charging Process

The computational model, originally created in 2004, is used to interpret the observations in terms of mesospheric dust particle parameters (Scales, 2004). In the modeling, the electron to ion temperature ratio during heating,  $T_e/T_i$  is varied in accordance with the heated center volume probed by the VHF radar. Two sets of simulations are designed to explain the experimental observations and the proposed approach for studying fundamental physics of the dust charging process in the PMSE region. All parameters are allowed to vary simultaneously in order to get the best agreement with the observations. The model imposes limitations on the parameters in order to produce the best correlation with the observations. A narrow range of parameters that are able to reproduce the observational results is determined. The model initialization is conducted using the observational data from recent in situ rocket measurements of dust particles within the cloud (Robertson et al., 2009). Several initial simulation runs are performed with the purpose of limiting the possible dust radius range in order to get the best agreement with the observations. The possibility of small dust

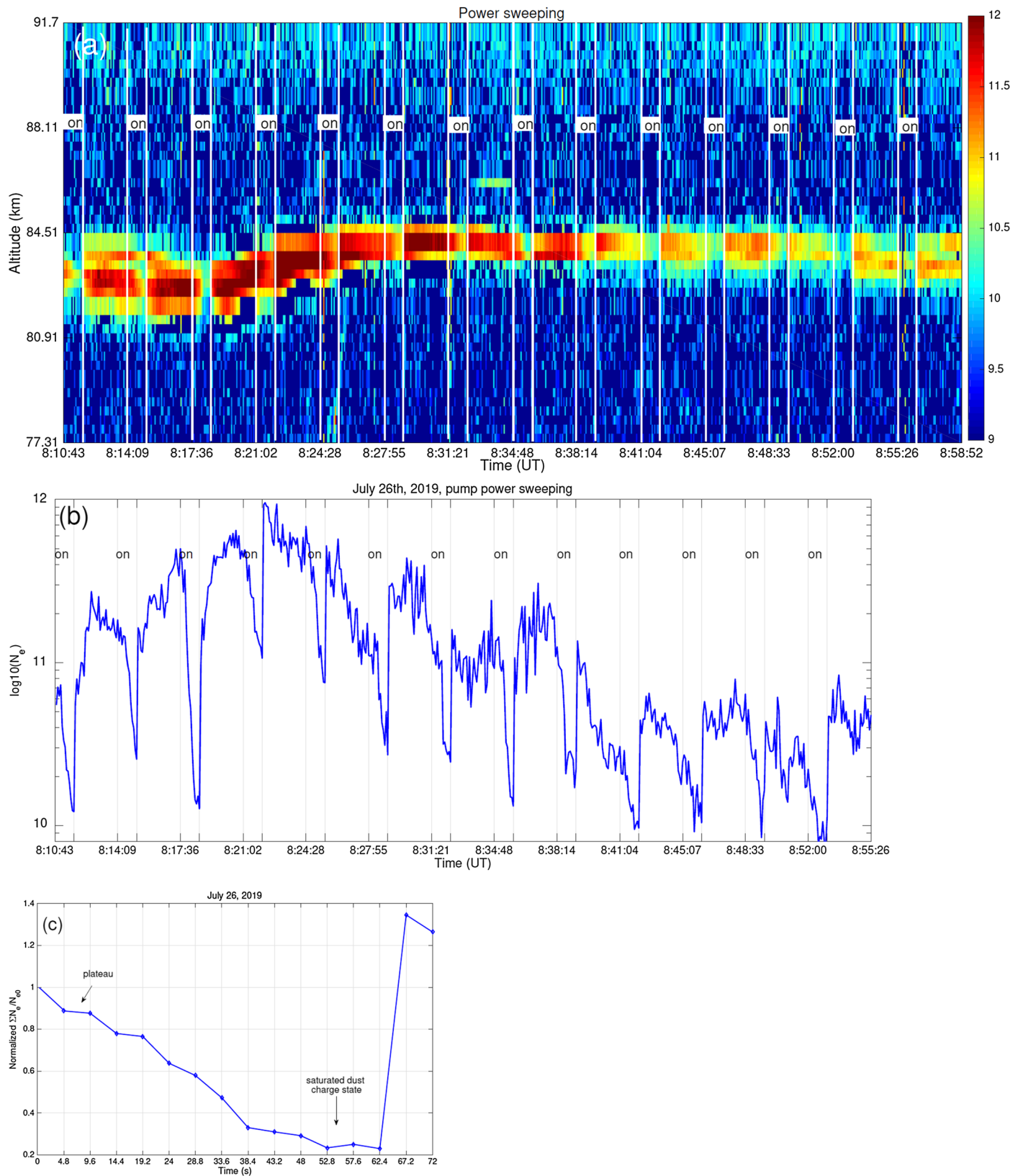


**Figure 3.** The HF pump power sweeping from 0 to 80 kW on 26 July 2019. (a) The backscattered signal is shown in  $\log_{10}(N_e)$  units. (b) Subintervals of quasi-continuous power variation associated with heating cycles shown in (a) (averaged within the PMSE altitude). (c) Averaged normalized radar echoes associated with all heating cycles.

particles, of the order of 1 nm, is excluded in this paper, as it requires a large density that is well beyond the typical densities in the associated region. Large dust particles (>5 nm) are also neglected due to the nature of the observation including stable background electron density, short duration of cloud appearance, and constant level of natural VHF PMSE throughout the observations. Therefore, dust radii of 3 and 4 nm are used in this study along with corresponding dust density and heating ratio to achieve the best consistency with the observations. The associated time evolution of the dust charge state during HF pump heating is also investigated.

Figures 4a and 4b denote the numerical results for  $r_d = 4$  nm,  $n_d/n_{e0} = 115\%$  corresponding to the observational data presented in Figures 2a and 2b. The dust fluctuation amplitude is assumed to be 50% of the background dust density. The cases shown in Figure 2a illustrate a 60% suppression of the VHF signal during HF heating at the HF power of 40 kW. The suppression level reaches  $\sim 80\%$  for 60 and 80 kW pump power levels. The turn-off overshoot discriminates the behavior of VHF PMSE during 60 and 80 kW heating. The best agreement between observations and simulations is obtained for  $T_e/T_i$  of 2.3, 2.8, and 2.9. The simulation results predict a turn-off overshoot of 5.5, 4.5, and 2.5 for HF pump of 80, 60, and 40 kW, respectively. The average charge state on dust particles ( $Z_{d,ave}$ ) shows an increase of average electron charge attached to dust particles by a factor of  $\sim 2$  associated with  $T_e/T_i$  of 2.8 and 2.9. A close comparison of radar echoes simulated by the model and time evolution of average dust charge reveals that the electron charging process dominated the diffusion process during radio-wave modulation and determines the final suppression level of the backscattered signal.

Figures 4c and 4d represent the numerical simulations for the experimental case of Figure 2c. According to the heating cycles shown in Figure 2c, the VHF PMSE drops 70%, 77.5%, and 85% at 40, 60, and 80 kW HF power, respectively. A small turn-off overshoot is observed in all cycles. The VHF PMSE during heater off period shows a temporal variation in the natural PMSE layer. This VHF PMSE evolution can be clearly seen in Figure 1c. This is mainly due to the change in the dust cloud parameters and can be attributed to the formation of new small dust particles. Such small particles are affected by the HF pump heating and electron charging process to a much lower degree. The red curve of 60 kW pump power in Figure 2c shows a greater pump-induced relaxation response of VHF PMSE after heating. The turn-off overshoot of 15% within 10 s of heater turn-off is observed. The numerical simulations match well the suppression behavior as well as the recovery to the initial value (red line in Figure 2c). The main feature observed in power stepping experiments is that there is a close agreement between the level VHF PMSE suppression and enhanced charge state. More suppression in the power level corresponds to higher dust charge state.

The heating cycle starting at the lowest HF pump of 10 kW on 24 July 2019 (Figure 2d) is analyzed in Figures 4e and 4f. The VHF PMSE during radio-wave heating shows a strong correlation with the heating powers of 10, 20, 40, 60, and 80 kW. A 20%,  $\sim 50\%$ , 70%, 76%, and 90% reduction of VHF PMSE during heating from the lowest to the highest powers was observed. The overall behavior of VHF PMSE after heater turn-off including a sudden increase to twice of the initial amplitude and remaining at that level is a clear manifestation of HF pump modulation. The behavior of VHF PMSE in the subsequent cycle at 80 kW is in agreement the corresponding trend of suppression level observed at 60 kW. As shown in Figure 2d, the rise time period of VHF PMSE after heater turn-off involves a sharp increase followed by a suppression of radar echo in some cases (e.g., for 80 kW in light green line) and continued with a slow recovery to the initial value. Two sets of parameters using 3 and 4 nm dust radius are performed. This could shed light on electron attachment onto dust particles and associated physics as well as dust particle characteristics. According to Figure 4f, the average charge state on the dust particles varies with approximately the same proportion at 3 and 4 nm associated with each pump power. The timing of the local maximum (turn-off overshoot) for both dust radii used in this study is in agreement with the experimental data. A close comparison of radar echo suppression level during radio heating, turn-off overshoot amplitude, and recovery of backscattered signal to normal level show that numerical results of 4 nm dust size (solid line in Figure 4e) produces the best agreement with the experimental observations. This approach will narrow the study of dust charging process with purpose of better understanding of charging rate. This goal will be achieved through the measured dust floating potential using the proposed technique.

One of the main characteristics of the observed VHF PMSE during continuous radio-wave modulation (Figure 3) is the plateau that is formed within the first few seconds of heating at low powers. This effect is attributed to the slow dust charging process due to small values of enhanced  $T_e/T_i$ . The plateau feature can

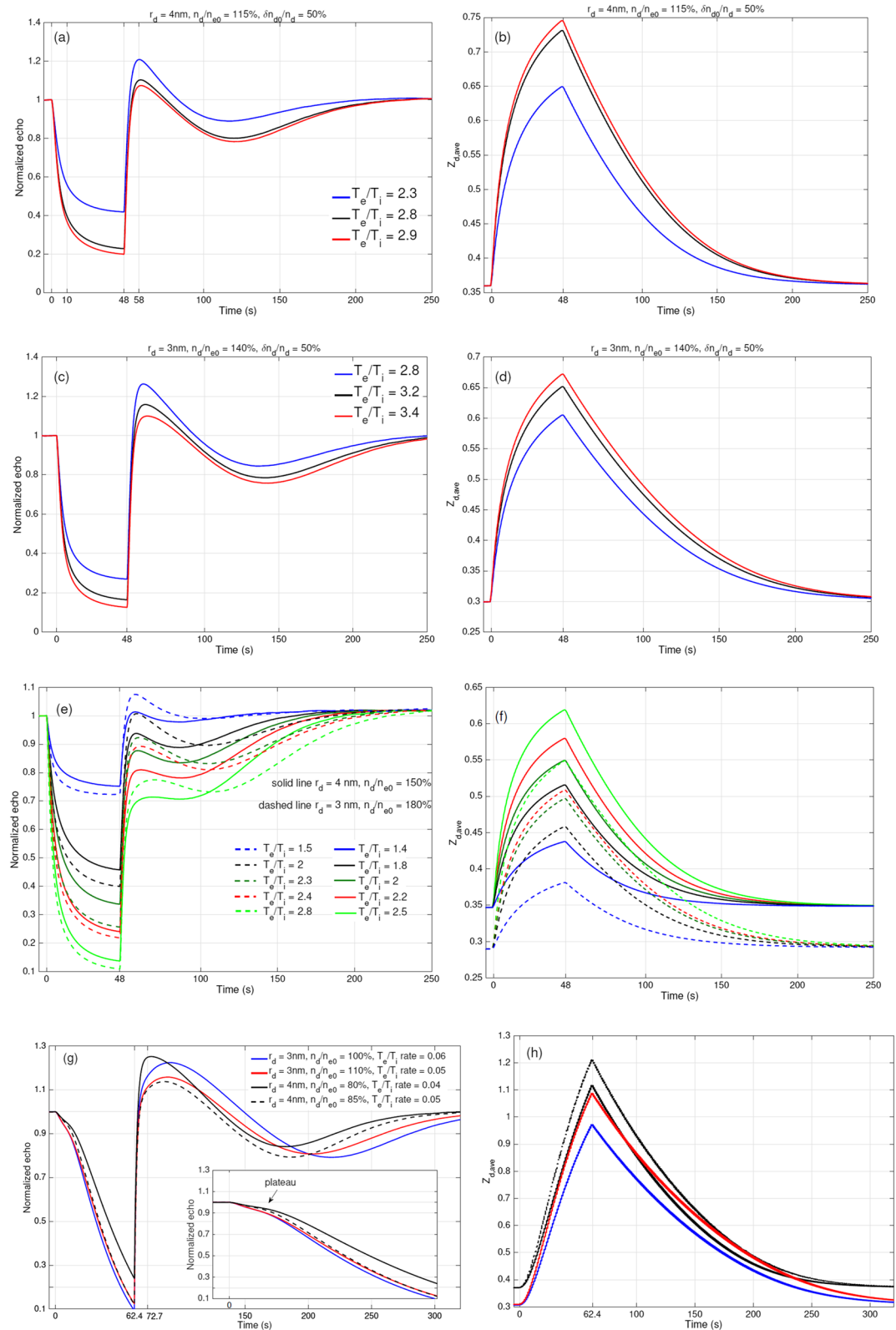


**Figure 4.** (a–f) Numerical results corresponding to experimental observations presented in Figures 1 and 2.  $Z_{d,ave}$  denotes the average electron charge on dust particles. The discrete HF pump variation and associated charge state simulated by the model are presented to characterize the similarity between VHF PMSE behavior and elevated dust simulated charge state. (g and h) Numerical results corresponding to experimental observations presented in Figure 3. The plateau feature formed in the numerical results corresponding to similar behavior in the observations is seen.



be implemented to determine the initial charge state on the dust particles. The numerical simulations based on two possible range of parameters are evaluated (Figures 4g and 4h). The main parameter used as the base of simulations is the dust radius. The continuous HF power variation included 120 steps from 0 to 80 kW during 62.4 s pump-on period. The computational model was set to increase the electron temperature ( $T_e$ ) similar to the experiment setup. The dust radius of 3 and 4 nm are used as the base of the simulations. The simulation results produce the plateau (10% reduction of VHF PMSE) within 16 s of heater turn-on associated with all parameters including the heating ratio. A close comparison reveals a plateau behavior of up to 10% within 10 s in the observations (Figure 3c). The suppression of radar echoes is estimated about 87% in comparison with the experimental data that show ~80% reduction. The clear saturated charging state is not seen in the simulation results. This could be due to modified recombination rate during heating that is a subject of future work. The turn-off overshoot amplitude also shows a good agreement. It should be noted that an average of 13 heating cycles over 1 hr of observations are compared with numerical simulations. Therefore, a small difference between the results is expected. The recovery of the radar echo to its initial value before turn-on emphasizes distinct variation in time that can be used to determine background parameters with high accuracy. According to Figure 4g, even small change in dust radius can introduce a notable footprint in the model curve. The echo strength data from continuously increasing the power shows a decrease that is related (to within a scaling constant) to the increase in charge state from the simulations. Therefore, the continuous and stepped power data together as a diagnostic can lead to direct observation of dust charging process in the PMSE source region.

## 5. Conclusion

The first radio-wave modulation of polar mesospheric summer echoes (PMSE) with varying HF pump power was conducted at EISCAT facility in Tromsø, Norway, in July 2019. The associated modulated PMSE was probed with a VHF radar at 224 MHz. The observations during pump power stepping as well as quasi-continuous HF power variation revealed the first direct signature of the dust charging process in the PMSE region. Numerical simulation is used in order to characterize the combination of quasi-continuous and discrete pump power variation. The model results are able to estimate the dust radius with 1 nm variation, dust density of 20% variation, and enhanced electron temperature with less than ~10% variation, which imposes a reliable limitation to estimate the background parameters. Moreover, the echo strength data from quasi-continuously increasing the pump power show a decrease that is related (to within a scaling constant) to the increase in charge state from the simulations. It has been shown that continuous HF pumping of the PMSE source region can be used to determine the initial and saturated charge state on the dust particles. While the unique experiment design is shown to be able to study the dust charging process in the mesosphere, more sophisticated experiments including switching back and forth between two HF pump powers as well as hysteresis increasing from a low to high pump power and vice versa could also lead to a determination of the charging rate. Such information, in addition to dusty plasma diagnosis, can provide a much better understanding of charging characteristics in the PMSE source region.

## Data Availability Statement

The data presented in this paper can be downloaded from the EISCAT online database (at <https://www.eiscat.se/scientist/data/>).

## Acknowledgments

EISCAT is an international association supported by research organizations in China (CRIRP), Finland (SA), Japan (NIPR and STEL), Norway (NFR), Sweden (VR), and the United Kingdom (NERC). A. M. would like to thank the University of Tehran for supporting this work. We thank Erik Varberg for assistance in implementing the experiments.

## References

- Chen, C., & Scales, W. A. (2005). Electron temperature enhancement effects on plasma irregularities associated with charged dust in the Earth's mesosphere. *Journal of Geophysical Research*, *110*, A12313. <https://doi.org/10.1029/2005JA011341>
- Chilson, P. B., Belova, E., Rietveld, M. T., Kirkwood, S., & Hoppe, U. (2000). First artificially induced modulation of PMSE using the EISCAT heating facility. *Geophysical Research Letters*, *27*, 3801–3804.
- Cho, J. Y. N., & Rottger, J. (1997). An updated review of polar mesosphere summer echoes: Observation, theory, and their relationship to noctilucent clouds and subvisible aerosols. *Journal of Geophysical Research*, *102*, 2001–2020.
- Ecklund, W. L., & Balsley, B. B. (1981). Long-term observations of the Arctic mesosphere with the MST radar at Poker Flat, Alaska. *Journal of Geophysical Research*, *86*, 7775–7780.
- Havnes, O., La Hoz, C., Nsheim, L. I., & Rietveld, M. T. (2003). First observations of the PMSE overshoot effect and its use for investigating the conditions in the summer mesosphere. *Geophysical Research Letters*, *30*(23), 2229. <https://doi.org/10.1029/2003JA010159>
- Havnes, O., Pinedo, H., La Hoz, C., Senior, A., Hartquist, T. W., Rietveld, M. T., & Kosch, M. J. (2015). A comparison of overshoot modeling with observations of polar mesospheric summer echoes at radar frequencies of 56 and 224 MHz. *Annales de Geophysique*, *33*, 737–747. <https://doi.org/10.5194/angeo-33-737-2015>

- Mahmoudian, A., Senior, A., Scales, W. A., Kosch, M. J., & Rietveld, M. T. (2018). Dusty space plasma diagnosis using the behavior of polar mesospheric summer echoes during electron precipitation events. *Journal of Geophysical Research: Space Physics*, *123*, 7697–7709. <https://doi.org/10.1029/2018JA025395>
- Rapp, M., & Lubken, F. J. (2004). Polar mesosphere summer echoes (PMSE): Review of observations and current understanding. *Atmospheric Chemistry and Physics*, *4*, 2601–2633.
- Rietveld, M. T., Senior, A., Markkanen, J., & Westman, A. (2016). New capabilities of the upgraded EISCAT high-power HF facility. *Radio Science*, *51*, 1533–1546. <https://doi.org/10.1002/2016RS006093>
- Robertson, S., Horny, M., Knappmiller, S., Sternovsky, Z., Holzworth, R., & Shimogawa, M. (2009). Mass analysis of charged aerosol particles in NLC and PMSE during the ECOMA/MASS campaign. *Annales de Geophysique*, *27*, 1213–1232.
- Scales, W. (2004). Electron temperature effects on small-scale plasma irregularities associated with charged dust in the Earth's mesosphere. *IEEE Transactions on Plasma Science*, *32*, 724.
- Scales, W. A., & Mahmoudian, A. (2016). Charged dust phenomena in the near Earth space environment. *Reports on Progress in Physics*, *79*(10), 106802. <https://doi.org/10.1088/0034-4885/79/10/106802>
- Senior, A., Mahmoudian, A., Pinedo, H., La Hoz, C., Rietveld, M. T., Scales, W. A., & Kosch, M. J. (2014). First modulation of high-frequency polar mesospheric summer echoes by radio heating of the ionosphere. *Geophysical Research Letters*, *41*, 5347–5353. <https://doi.org/10.1002/2014GL060703>